

1 **Identification of hydrocarbon sulfonates as previously overlooked transthyretin**
2 **ligands in the environment**

3

4 Yufeng Gong¹, Jianxian Sun¹, Holly Barrett¹, Hui Peng^{*1,2}

5

6

7 ¹Department of Chemistry, University of Toronto, Toronto, ON, Canada, M5S 3H6

8 ²School of the Environment, University of Toronto, Toronto, ON, Canada, M5S 3H6

9

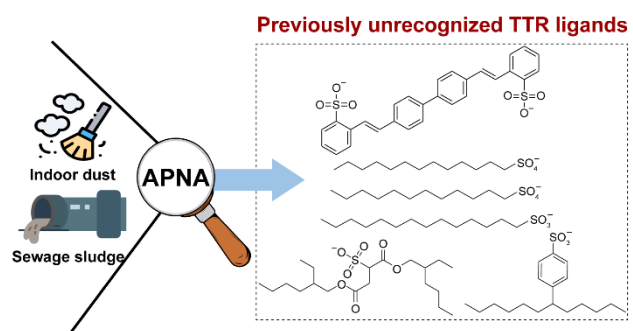
10

11 ***Corresponding authors:** Dr. Hui Peng, hui.peng@utoronto.ca, Department of
12 Chemistry, University of Toronto, Toronto, ON, M5S 3H6, Canada.

13

14

15 TOC



16

17

18

19 **Abstract**

20 Incidences of thyroid disease, which has long been hypothesized to be partially
21 caused by exposure to thyroid hormone disrupting chemicals (TDCs), have rapidly
22 increased in recent years. However, only ~1% of the binding activity of human
23 transthyretin (hTTR), an important thyroid hormone transporter protein, can be
24 explained by known TDCs. In this study, we aimed to identify the major hTTR ligands
25 in Canadian indoor dust and sewage sludge by employing protein-guided nontargeted
26 analysis. hTTR binding activities were detected in all 11 indoor dust and 9 out of 10
27 sewage sludge samples (median 458 and 1134 $\mu\text{g T}_4/\text{g}$ in dust and sludge, respectively)
28 by the FITC- T_4 displacement assay. Through employing protein Affinity Purification
29 with Nontargeted Analysis (APNA), 31 putative hTTR ligands were detected including
30 perfluorooctane sulfonate (PFOS). Two of the most abundant ligands were identified as
31 hydrocarbon surfactants (e.g., dodecyl benzenesulfonate), which were confirmed by
32 authentic chemical standards. Structure-activity relationships (SAR) of hydrocarbon
33 surfactants were explored by investigating the binding activity of 11 hydrocarbon
34 surfactants to hTTR. Optimal carbon chain length (C_{12-14}) was found to achieve a high
35 binding affinity. By employing *de novo* nontargeted analysis, another abundant ligand
36 was surprisingly identified as a di-sulfonate fluorescent brightener, 4,4'-Bis(2-
37 sulfostyryl)biphenyl sodium (CBS). CBS was validated as a nM-affinity hTTR ligand
38 with an IC_{50} of 345 nM. In total, hydrocarbon surfactants and fluorescent brightener
39 could explain 1.92-17.0% and 5.74-54.3% of hTTR binding activities in dust and sludge
40 samples, respectively, whereas PFOS only contributed <0.0001% to the activity. Our
41 study revealed for the first time that hydrocarbon sulfonates are previously overlooked
42 hTTR ligands in the environment.

43

44 **Keywords:** TTR; Hydrocarbon surfactants; CBS; Nontargeted analyses; Bioanalytical
45 equivalent concentration

46 **Synopsis:** Hydrocarbon surfactants and fluorescent brightener are previously
47 overlooked TTR ligands in the environment.

48

49 **Introduction**

50 Thyroid hormones (THs) play a pivotal role in regulating many physiological
51 processes in organisms such as growth, development, and energy metabolism.¹
52 Disruption of THs levels can impact the development of the central nervous system,
53 especially during fetal development,² and is associated with neurological disorders
54 including Alzheimer's disease (AD)³. Epidemiological studies have revealed an
55 association between exposure to thyroid hormone disrupting chemicals (TDCs) and the
56 increased risk of thyroid-related diseases.⁴⁻⁶ Transthyretin (TTR) is a major thyroxine
57 (T₄) transport protein in serum that has been demonstrated to mediate the toxicity of
58 many TDCs. TDCs can compete with endogenous T₄ for binding to TTR, which can
59 lead to the increased clearance of free T₄ and the disruption of THs homeostasis.^{7, 8} In
60 addition to THs disruption, binding to TTR can also mediate the transport of chemical
61 pollutants across placental and blood-brain barriers into various compartments (*e.g.*,
62 fetus and brain), which may induce a multitude of adverse effects.⁹⁻¹¹ Thus, the
63 identification of environmental chemicals binding to TTR is important for
64 understanding their potential health risks.

65 TTR is a tetramer protein with a large binding pocket in the middle channel. Multiple
66 compound classes have been reported to bind to TTR, including hydroxylated
67 polybrominated diphenyl ethers (OH-PBDEs)¹², phenolic disinfection products
68 (phenolic-DBPs)¹³, hydroxylated and sulfated metabolites of polychlorinated biphenyls
69 (PCBs)¹⁴, per- and polyfluoroalkyl substances (PFASs)¹⁵, and many others.¹⁶ Despite
70 the extensive studies on TTR, known environmental TTR ligands (*e.g.*, PFASs) can
71 only explain 1.2% of the total TTR activity of house dust¹⁷, while the vast majority of
72 TTR ligands in the environment remain unidentified. This knowledge gap should
73 largely result from the vast number of synthetic chemicals manufactured worldwide
74 (>350,000 until 2019)¹⁸ and the limited capacity of conventional toxicity testing
75 methods. Effect-directed analysis (EDA) is a promising tool for the identification of
76 unknown toxic compounds in complex environmental matrices.¹⁹ However, EDA is
77 time-consuming and, more importantly, is prone to high false discovery rates due to the
78 co-elution of chemicals in the same fractions. For example, although strong TTR

79 binding activity was detected for a standard dust sample (SRM 2585), TTR ligands
80 identified by EDA (e.g., synthetic musks, PFASs, and organophosphates) could barely
81 explain the total effects.²⁰ Similarly, triclosan and nonylphenol were demonstrated to
82 contribute to the TTR binding activity of a sediment sample by EDA, but only <1% of
83 the activity could be explained.²¹ Together, these results underscore the need to
84 systematically identify unknown TTR ligands in the environment.

85 Individual testing of each of the 350,000 compounds for TTR activity is infeasible
86 due to the significant cost requirement and the unavailability of standards. To address
87 this challenge, we have developed a “top-down” approach termed “protein Affinity
88 Purification with Nontargeted Analysis (APNA)”^{22, 23} for the identification of ligands
89 at the exposome-wide level. The APNA method is fundamentally different from
90 conventional EDA methods in that it uses protein affinity to directly isolate bioactive
91 chemicals from environmental mixtures in an unbiased manner. To date, APNA has
92 been successfully applied to identify novel ligands binding to human nuclear
93 receptors,^{24, 25} transport proteins,^{26, 27} and even bacterial enzymes^{28, 29}. Inspired by those
94 successful applications, we herein employed the APNA method to systematically
95 identify human TTR (hTTR) ligands in indoor dust and sewage sludge samples.
96 Surprisingly, hydrocarbon sulfonates including surfactants and a fluorescent brightener
97 (*i.e.*, 4,4'-Bis(2-sulfoxy)styryl)biphenyl sodium (CBS)), were identified as major hTTR
98 ligands in the environment, highlighting the need to re-evaluate their chemical safety
99 in the future.

100

101 **Materials and Methods**

102 **Chemicals and Reagents.** Authentic standards including several hydrocarbon
103 surfactants, perfluorooctanesulfonic acid (PFOS), thyroxine (T₄), rosiglitazone, and
104 fluorescein isothiocyanate (FITC) (isomer I) were purchased from Sigma-Aldrich
105 (Oakville, ON, CA). Docusate sodium and sodium tridecyl sulfate were obtained from
106 Chem Service (West Chester, PA, USA). CBS was obtained from Alfa Chemistry
107 (Ronkonkoma, NY, USA). Detailed information regarding the chemical standards is
108 provided in [Table S1](#) of the [Supporting Information \(SI\)](#). Native hTTR protein purified

109 from human plasma (purity \geq 95%) was obtained from Sigma-Aldrich (Catalog#: 110 529577; Oakville, ON, CA). LC-MS grade acetonitrile, methanol, water, and 111 ammonium acetate were purchased from Fisher Scientific (Ottawa, ON, CA).

112 **Environmental sample collection and extraction.** A total of 11 indoor dust samples 113 and 10 sewage sludge samples were collected and extracted as previously described.²⁶ 114 Detailed information on the sample preparation is provided in the [SI](#).

115 **FITC-T₄ Displacement Assay.** The binding affinities of pulled-out chemicals or 116 extracts of environmental samples to hTTR were determined individually by a 117 fluorescein–thyroxine (FITC-T₄) displacement assay. Synthesis of the fluorescence 118 probe FITC-T₄ and development of the displacement assay were completed according 119 to previous studies with minor modifications,^{30, 31} and a detailed description of the 120 method is provided in the [SI](#). For extracts of indoor dust and sewage sludge, the 121 uppermost concentration was capped at 0.5 g/L due to the significant signal interference 122 caused by the intense coloration of the extracts at exposure concentrations exceeding 123 0.5 g/L. It should be noted that the native form of hTTR protein, purified directly from 124 human plasma rather than the recombinant His-tagged hTTR from *E. coli*, was used for 125 the assay to cross-validate the APNA results in order to avoid the impact of the His tag 126 on potential binding activities.

127 **Overexpression of Recombinant His-hTTR Protein.** In this study, the His-tagged 128 hTTR protein was expressed in *E. coli* BL21 (DE3) cells (Novagen, WI, USA). The 129 expression vector of human His-tagged TTR protein was obtained from GenScript 130 corporation (Piscataway, NJ, USA). More details are provided in the [SI](#).

131 **Protein Affinity Pulldown.** In this study, the APNA method^{22, 24-26} was employed to 132 identify environmental pollutants binding to hTTR in indoor dust and sewage sludge. 133 In brief, crude lysates (250 μ L) of *E. coli* cells overexpressing His-tagged hTTR protein 134 were incubated with 3 μ L of sample extract (*i.e.*, indoor dust or sewage sludge) in a 96- 135 well plate. 5 μ L of His-select nickel magnetic agarose beads (H9914, Sigma-Aldrich) 136 were then added and the whole plate was incubated at 4 °C for 30 min in a rotator at 20 137 rpm to allow the formation of protein-ligand complexes. The experiments were 138 performed in triplicate ($N = 3$). Lysates of wild-type *E. coli* cells were used as negative

139 controls. After incubation, the 96-well plate was placed on a magnetic field plate to
140 separate the beads. The supernatant was removed, and the magnetic beads were washed
141 3 times using 100 μ L of wash buffer (50 mM Tris, 300 mM sodium chloride, and 30
142 mM imidazole, pH 8.0). Then, 100 μ L of elution buffer (50 mM Tris, 300 mM sodium
143 chloride, and 300 mM imidazole, pH 8.0) was added to wash-off the protein-ligand
144 complex from the magnetic beads. The eluted solution was then transferred to a ZebaTM
145 spin 7k MWCO desalting plate (Thermo Fisher Scientific). Following centrifugation at
146 1000 g for 2 minutes, the eluted solution was collected and transferred to a 1.5 mL
147 Eppendorf tube. The sample was then dried down by a speed vacuum at room
148 temperature and 100 μ L of cold methanol was added to denature the His-tagged hTTR
149 protein. The sample was vortexed for 1 minute, and centrifuged again for 30 minutes at
150 14,000 g. The supernatant was finally transferred to sample vials for LC-MS/MS
151 analysis.

152 **Ligand Identification by Nontargeted Analyses.** LC-MS/MS analysis was
153 conducted by use of a Q Exactive mass spectrometer coupled online with a Vanquish
154 ultra-high-performance liquid chromatography (UHPLC) system (Thermo Fisher
155 Scientific, Waltham, MA, USA). Complete details of the instrument methods are
156 provided in the SI. Nontargeted analyses were accomplished with an in-house R
157 program as described in our previous studies.³² A putative lock mass algorithm (PLMA)
158 was applied for post-acquisition calibration of mass spectra before peak picking.³² The
159 ‘XCMS’ R package³³ was used for peak detection with a mass tolerance of 2.5 ppm.
160 The peak features were aligned across samples with a mass tolerance of 2.5 ppm and
161 retention time window of 20 seconds after retention time adjustment. In this study, to
162 ensure specificity, lysates of wild-type *E. coli* cells were used as the negative control.
163 The ratio between the peak abundance from *E. coli* overexpressing His-tagged hTTR
164 to that from wild-type *E. coli* was calculated for each peak feature. The *P* value of the
165 difference between the two groups was also determined by student’s t-test. Only the
166 features exhibiting greater peak intensities (fold change > 5, *p* value < 0.05) in the
167 overexpressed hTTR group compared to the wild-type *E. coli* group were considered
168 as potential ligands. *E. coli* overexpressing His-tagged hTTR without incubation with

169 dust/sludge extracts was also employed as a second negative control. The pulled-out
170 LC-MS features were further filtered by using the second negative control with the
171 same cutoffs. Isotopic peaks and adducts were excluded by matching chromatographic
172 peaks and theoretical mass differences. The final differentiated peak list from the output
173 of the R program was manually checked by use of Qual Browser in Xcalibur software.
174 Then, the differentiated peaks were searched against the United States Environmental
175 Protection Agency (U.S. EPA) Toxic Substances Control Act Chemical Substance
176 Inventory (TSCA Inventory)³⁴ and the Network of Reference Laboratories, Research
177 Centers, and Related Organizations for Monitoring of Emerging Environmental
178 Substances (NORMAN) Suspect List Exchange database³⁵ using an in-house R
179 program.³² A mass tolerance of 2.5 ppm was used. Confidence levels were assigned to
180 all identities according to the Schymanski scale.³⁶

181 **Absolute quantification.** The concentrations of identified hTTR ligands were
182 determined by LC-MS/MS in this study. External calibration curves were constructed
183 for each chemical by using corresponding authentic standards. Please see the [SI](#) for
184 more details.

185 **Molecular docking.** AutoDock Vina 1.1.2³⁷ was used to predict the binding modes
186 of identified chemicals to hTTR (PDB code: 2ROX). The detailed procedures and
187 parameters are available in the [SI](#).

188 **Calculation of BEQ.** In this study, the contribution of the identified hTTR ligands
189 to the hTTR binding activities of environmental samples was estimated by comparing
190 the bioanalytical equivalent concentration (BEQ) from bioanalysis (BEQ_{bio}) and the
191 BEQ from chemical analysis (BEQ_{chem}).⁴ The BEQ_{bio} of environmental samples toward
192 hTTR binding were estimated on the basis of IC₅₀ values determined by the FITC-T₄
193 displacement assay, with T₄ as a reference compound, using eq 1.

$$194 \quad \text{BEQ}_{\text{bio}} = \frac{\text{IC}_{50(\text{T}_4)}}{\text{IC}_{50(\text{environmental samples})}} \quad (1)$$

195 To calculate the BEQ_{chem}, the relative potency (REP_i) of each tested chemical (i) relative
196 to T₄ was estimated on the basis of its IC₅₀ using eq 2.

197
$$\text{REP}_i = \frac{\text{IC}_{50(\text{T}_4)}}{\text{IC}_{50(i)}} \quad (2)$$

198 Then, the BEQ_{chem} was estimated by multiplying the quantified concentrations of each
199 chemical (C_i) in the environmental samples by their respective REP values (eq 3).

200
$$\text{BEQ}_{\text{chem}} = \sum_{i=1}^n \text{REP}_i \times C_i \quad (3)$$

201 Finally, the contributions to the observed hTTR binding activities were determined by
202 eq 4:

203
$$\text{Contribution (\%)} = \frac{\text{BEQ}_{\text{chem}}}{\text{BEQ}_{\text{bio}}} \times 100\% \quad (4)$$

204 Please refer to [SI](#) for more details about statistics.

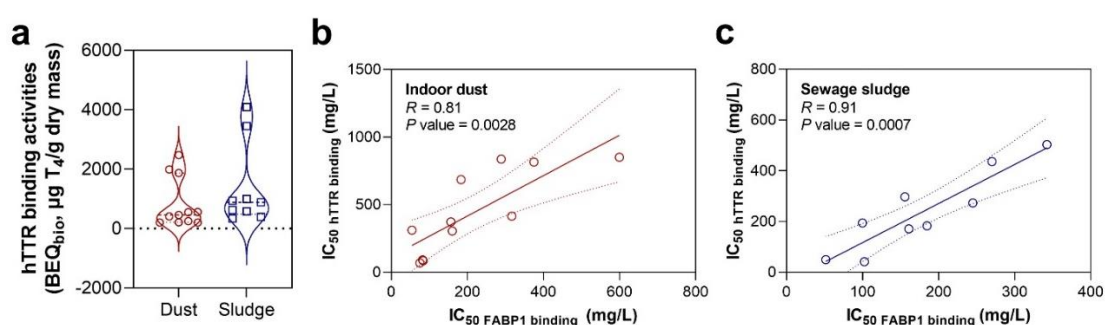
205

206 **Results and Discussion**

207 **Widespread hTTR binding activities in indoor dust and sewage sludge.** To
208 investigate the potential occurrence of hTTR ligands in the environment, we employed
209 the FITC-T₄ probe-based fluorescence displacement assay developed in previous
210 studies.^{30, 38} The FITC-T₄ probe shows a fluorescence enhancement at 518 nm when
211 binding to the hTTR protein, probably due to the impact on the intersystem crossing
212 effect of the iodine atom. If a competitive hTTR ligand is present, the probe would be
213 displaced from hTTR, resulting in a decrease in the fluorescence signal.³⁰ The FITC-T₄
214 probe was synthesized using a one-step amine coupling reaction followed by a GPC
215 column purification. The identity and purity (>99%) of the probe was confirmed by
216 high resolution mass spectrometry ([Figure S1a](#) and [S1b](#)). To test its function, the
217 synthesized probe was incubated with native hTTR protein for fluorescence
218 measurement. The fluorescence intensity at 518 nm increased with increasing
219 concentrations of FITC-T₄ and reached saturation at about 1 μM of FITC-T₄ when
220 incubating with a fixed concentration (1 μM) of hTTR ([Figure S1c](#)). To further
221 benchmark the assay for competitive ligand screening, three well-known hTTR ligands
222 (*i.e.*, thyroid hormone T₄, 6-OH-BDE-47, and PFOS) were individually incubated with
223 the FITC-T₄ probe (130 nM) and hTTR protein (90 nM). As expected, all three

224 chemicals displaced the FITC-T₄ probe from hTTR protein as evidenced by the
225 decrease in the fluorescence signal in a dose-dependent manner (Figure S2). Moreover,
226 the REP values of 6-OH-BDE-47 (REP = 1.83) and PFOS (REP = 0.49) relative to T₄
227 measured in our study are comparable to those reported in previous studies (REP of 2
228 and 0.4 for 6-OH-BDE-47³⁹ and PFOS,¹⁷ respectively), demonstrating the validity of
229 the synthesized FITC-T₄ probe.

230



231

232 **Figure 1. Widespread hTTR binding activity in the environment.** (a) Detected
233 hTTR binding activities of indoor dust and sewage sludge extracts expressed as BEQ_{bio}
234 (µg T₄/g dry mass). (b) and (c), correlation analysis of the binding activities between
235 hTTR and FABP1 across indoor dust and sewage sludge extracts, respectively. The
236 hTTR binding activity was determined by a FITC-T₄ fluorescence displacement assay.
237 N = 3. All data were normalized to solvent control. The FABP1 binding potencies were
238 adopted from a previous study.²⁶

239

240 We then moved forward to use the FITC-T₄ displacement method for the
241 measurement of hTTR activity in environmental extracts. A total of 11 indoor dust
242 samples and 10 sewage sludge samples were extracted and tested for their hTTR
243 binding potencies. Except for one sludge sample (*i.e.*, sludge sample S5), all the
244 extracted indoor dust and sewage sludge samples showed marked hTTR binding
245 activities, as depicted by the full dose-response curves in Figure S3 and S4. The T₄-
246 BEQ_{bio} concentrations of the indoor dust extracts were estimated to be 201 to 2477 µg/g
247 dust (median: 458 µg/g dust), while those of sewage sludge extracts were higher (range:
248 340 to 4089 µg/g sludge; median: 881 µg/g sludge) (Figure 1a and Table S2). The strong
249 hTTR binding activity of indoor dust samples was not surprising as extensive hTTR
250 binding activity has been previously reported for dust samples collected from Japan and

251 the United States.^{17, 40, 41} Wastewater-based monitoring has long been used as a
252 promising tool to measure the collective consumption or chemical exposure of
253 humans.⁴² The sewage sludge samples were collected from two biggest wastewater
254 treatment plants in Toronto, and thus the strong hTTR binding activity of the sewage
255 sludge extracts suggested the potential population-wide exposure of TDCs to the
256 Toronto population.

257 In our recent study, the binding activities of human liver fatty acid binding protein 1
258 (FABP1) and peroxisome proliferator-activated nuclear receptor γ (PPAR γ) ligand
259 binding domain (LBD) which are important target proteins of environmental obesogens
260 were also determined for the same dust and sludge samples.²⁶ This provided an
261 opportunity to compare the binding activities of three proteins (*i.e.*, hTTR, FABP1, and
262 PPAR γ) across the samples. A significantly positive correlation was observed between
263 the hTTR binding activities and the FABP1 binding activities across indoor dust ($R =$
264 0.81 , $P = 0.0028$, [Figure 1b](#)) and sewage sludge ($R = 0.91$, $P = 0.0007$, [Figure 1c](#))
265 samples. Positive correlation was also observed between hTTR and PPAR γ LBD but
266 the correlation was weaker ([Figure S5](#)). The results demonstrated that these three
267 proteins might share common ligands in the environment, particularly between hTTR
268 and FABP1. This is very interesting, as hTTR and FABP1 are both major transport
269 proteins, and they have been reported to share some common endogenous ligands (*e.g.*,
270 arachidonate).^{43, 44}

271 **Nontargeted identification of hTTR ligands by APNA.** To identify the primary
272 hTTR ligands in the environmental samples, the APNA approach was employed. The
273 His-tagged hTTR was overexpressed in *E. coli* and its amino acid sequence was verified
274 by LC-MS/MS ([Figure S6](#)). For proof of concept, the APNA method was first
275 benchmarked by incubating a mixture of T₄ and 6-OH-BDE-47 with recombinant His-
276 tagged hTTR protein. As shown in [Figure S7a](#), these two well-known hTTR ligands,
277 with binding affinities at nanomolar range (*i.e.*, T₄ and 6-OH-BDE-47³⁰), were
278 significantly pulled-out by His-tagged hTTR but not by the wild-type *E. coli* lysates.
279 Meanwhile, in another independent validation experiment, the mixture of T₄ and
280 rosiglitazone were tested against three different protein targets, including His-tagged

281 hTTR, His-tagged FABP1, and His-tagged PPAR γ LBD, separately. As expected, T₄
282 and rosiglitazone were only pulled-out by their corresponding target proteins (i.e., T₄
283 for hTTR; rosiglitazone for FABP1 and PPAR γ LBD), demonstrating the high
284 selectivity of the APNA approach (Figure S7b). These results together demonstrated
285 that the APNA approach can be used to isolate hTTR ligands with good selectivity.

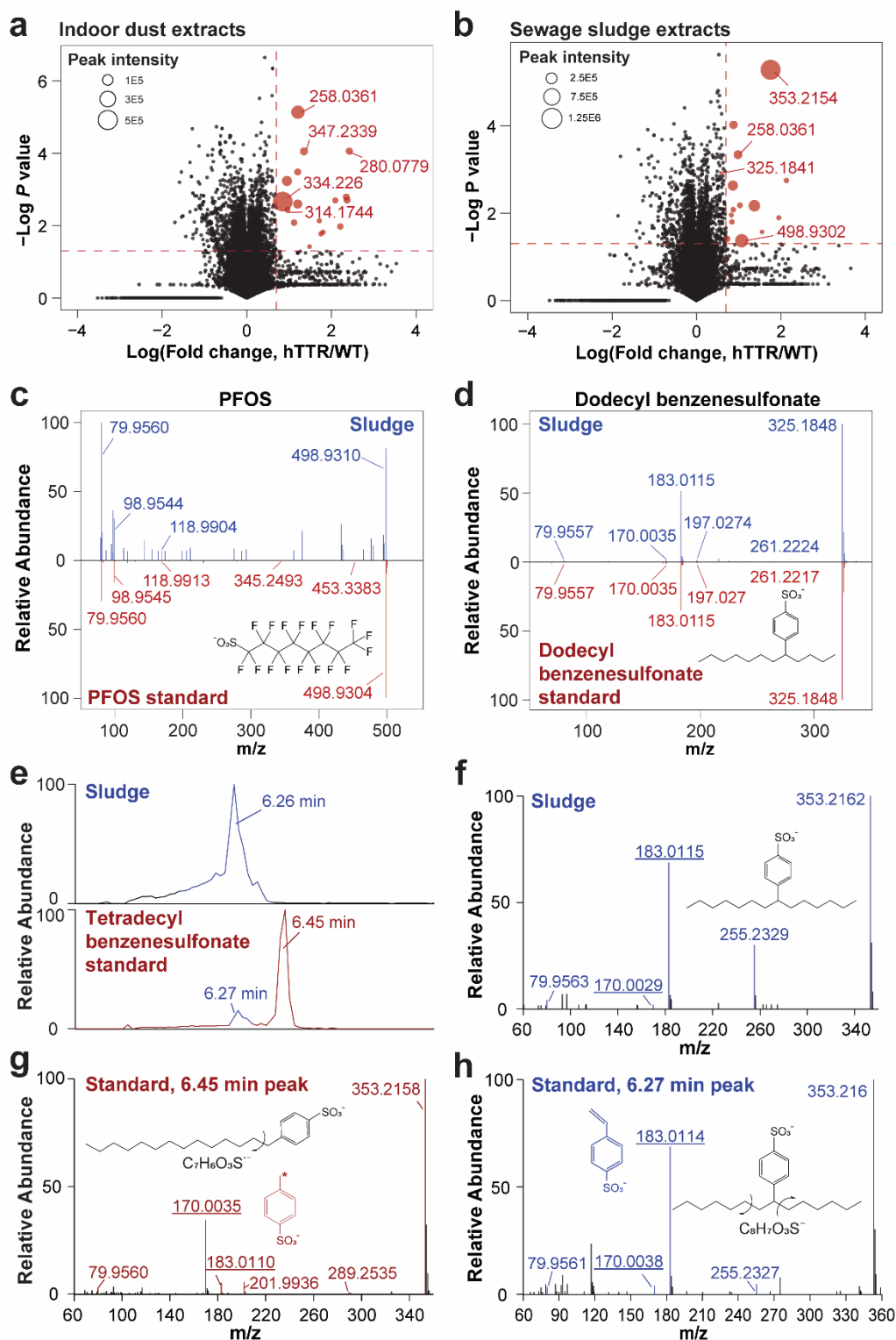
286 Subsequently, we employed the APNA method to directly identify environmental
287 hTTR ligands from the indoor dust and sewage sludge extracts containing thousands of
288 co-occurring chemicals. Among the 19,175 and 19,028 LC-MS features detected in
289 pooled indoor dust and sewage sludge extracts, respectively, 17 and 14 features were
290 specifically pulled-out by the *E. coli* lysates overexpressing His-tagged hTTR with >5-
291 fold higher abundances than the wild-type *E. coli* lysates (negative control) ($P < 0.05$;
292 Figure 2a and 2b). The peak shapes, m/z , and retention times (RTs) of all the pulled-out
293 features were confirmed by manual inspection. During the data inspection stage, one
294 additional feature (i.e., $m/z = 325.1841$, RT = 5.86 min), which was found to be
295 significantly pulled-out by His-tagged hTTR protein ($P < 0.005$) but with a lower fold
296 change (fold change = 3.82) due to its high background in the LC-MS instrument, was
297 manually added to the pulled-out list. After removing the repetitive features, a total of
298 31 nonredundant LC-MS features were detected as putative hTTR ligands across the
299 dust and sludge extracts (Table S3).

300 Through suspect screening against the TSCA Inventory database and the NORMAN
301 database, the structures of 3 LC-MS features were tentatively assigned, including PFOS
302 ($m/z = 498.9302$, RT = 5.02 min, [C₈F₁₇O₃S]⁻, mass error = -0.035 ppm) (Figure 2c).
303 The detection of PFOS as a hTTR ligand was not surprising since its hTTR binding
304 activity has been widely verified in previous studies by several different approaches
305 such as TTR binding assays with FITC-T₄⁴⁵ or ¹²⁵I-labeled T₄¹⁵ and *in silico* modeling⁴⁶.
306 These results verified our APNA method for the identification of hTTR ligands from
307 environmental mixtures. However, some well-known hTTR ligands, such as OH-
308 PBDEs,^{39, 47} were not detected by the APNA method which was likely due to their
309 extremely low concentrations in environmental samples (typically at low ng/g levels⁴⁸).
310 Indeed, even PFOS exhibited a peak intensity that was several orders of magnitude

311 lower than that of other putative ligands. This indicated that previously known hTTR
312 ligands might contribute only minorly to the hTTR activity, which was consistent with
313 a previous study which demonstrated that known chemicals only explained 1.2% of
314 hTTR activity in indoor dust.¹⁷

315 We then moved forward to assign the structures of other previously unknown hTTR
316 ligands. By searching against the TSCA database, the ligands $m/z = 325.1841$ and m/z
317 $= 353.2154$ were assigned as dodecyl benzenesulfonate and tetradecyl
318 benzenesulfonate, respectively. Their identities were supported by the detection of a
319 characteristic MS² fragment of $m/z = 183.0113$ ($[\text{C}_8\text{H}_7\text{O}_3\text{S}]^-$, mass error = -0.738 ppm)
320 corresponding to the ethylene-substituted benzenesulfonate.^{49, 50} Moreover, the
321 fragment ion $m/z = 79.9560$ ($[\text{SO}_3]^-$, mass error = -1.363 ppm) further suggested they
322 contained a sulfonate group. The identity of $m/z = 325.1841$ was confirmed as dodecyl
323 benzenesulfonate by comparing its MS² spectrum with that of an authentic standard
324 (Figure 2d). However, as shown in Figure 2e, the RT of the other putative ligand $m/z =$
325 353.2154 from the sample extracts (RT = 6.26 min) did not match to the standard of
326 tetradecyl benzenesulfonate (RT = 6.45 min). After careful inspection, the MS²
327 spectrum of the putative ligand was found to be similar to that of the standard, yet the
328 relative intensities of fragments $m/z = 183.0113$ and $m/z = 170.0038$ were different
329 (Figure 2f and g). This demonstrated that the putative ligand might be an isomer of
330 tetradecyl benzenesulfonate, as alkylbenzene sulfonates are known to be manufactured
331 as a mixture of many isomers. Indeed, we noted that the retention time (RT = 6.27 min)
332 and MS² spectrum of the minor peak of the tetradecyl benzenesulfonate standard
333 matched to the tentative ligand (Figures 2h). Collectively, we concluded that the
334 putative ligand $m/z = 353.2154$ should be the internal/branched isomer of tetradecyl
335 benzenesulfonate due to the fact that 1) branched isomers of compounds are known to
336 elute earlier than their linear isomers (*i.e.*, the standard of tetradecyl benzenesulfonate)
337 on reversed-phase columns,⁵¹ and 2) the dominance of the MS² fragment $m/z =$
338 183.0113 from the branched isomer might be generated through the radical-induced
339 cleavage of the branched side chain.

340



342

343 **Figure 2. Identification of hTTR ligands by APNA.** (a) and (b) Volcano plots
 344 representing the log-transformed fold changes and corresponding P values of each LC-
 345 MS feature detected in the pooled indoor dust and sewage sludge extracts. Red dots
 346 indicate LC-MS features having significantly greater abundances (fold change >5 , $P <$
 347 0.05) in *E. coli* lysates overexpressing His-tagged hTTR protein than the negative

348 control. Isotopic features and adducts were removed. Dot size (only for the upper right
349 quadrant) represents the peak intensity for each pulled-out compound. (c) and (d) MS²
350 spectra of PFOS and dodecyl benzenesulfonate, respectively, from sludge samples and
351 matching to authentic standards. (e) Retention time of putative ligand $m/z = 353.2154$
352 matching to an authentic standard of tetradecyl benzenesulfonate. (f), (g), and (h) MS²
353 spectra of putative ligand $m/z = 353.2154$, major peak in the standard (RT = 6.45 min),
354 and minor peak in the standard (RT = 6.27 min). For the two alkylbenzene sulfonates,
355 pictured above is one potential isomer for each compound, of which there are many
356 possible isomers.

357

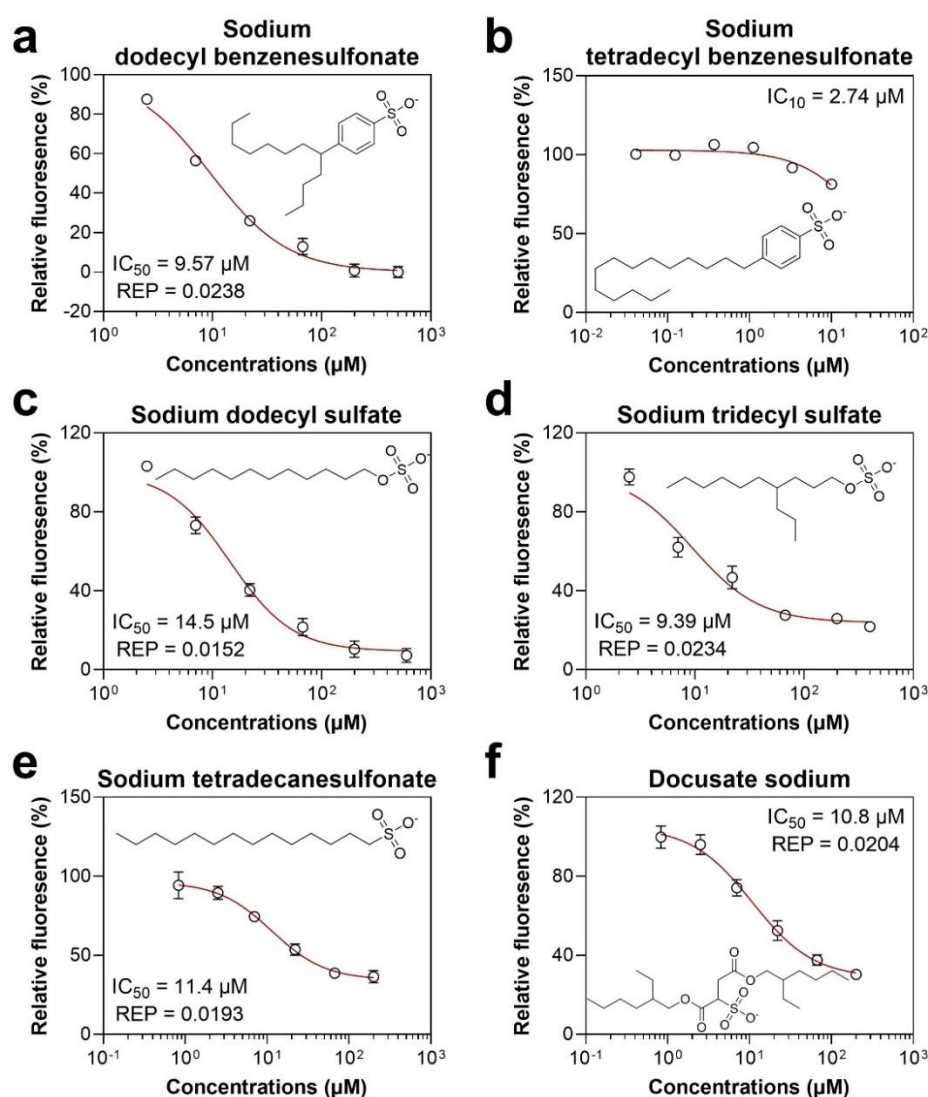
358 Overall, two major hTTR ligands were identified as hydrocarbon sulfonates.
359 Identification of hydrocarbon sulfonates as hTTR ligands was unexpected but not
360 completely surprising, as their structures are similar to PFOS. Hydrocarbon sulfonates
361 are widely used as anionic surfactants in various household, industrial, and institutional
362 applications. For instance, they appear in cleaner, lubricating agent, emulsifier, paint
363 additives, and opacifer with an annual aggregated product volume of 100,000 to
364 500,000 pounds in the United States, for just dodecyl benzenesulfonate alone,
365 according to Chemical Data Reporting (CDR).⁵² Due to their high production
366 volumes and wide applications, these compounds have been detected in indoor dust and
367 sewage sludge samples at extremely high concentrations (mg/g levels), at ~6 orders of
368 magnitude higher than those of PFOS in the same samples.²⁶

369 **Evaluation of hTTR binding activities of hydrocarbon surfactants.** We further
370 employed the FITC-T₄ displacement assay to cross-validate the binding activity of
371 these newly identified hTTR ligands by using their commercially available standards.
372 In line with the APNA results, dodecyl benzenesulfonate showed strong binding
373 potency to hTTR with the IC₅₀ and REP values of 9.57 μM and 0.0238, respectively
374 (Figure 3a), whereas the hTTR binding activity of tetradecyl benzenesulfonate was
375 much weaker in that only an IC₁₀ value could be determined (IC₁₀ = 2.74 μM; Figure
376 3b). It should be noted that the hTTR binding potency of tetradecyl benzenesulfonate
377 was obtained by a linear/external isomer, not the branched/internal isomer (not
378 commercially available) which was initially pulled-out from environmental samples by
379 the hTTR protein. Previous studies have reported the stronger protein binding activities

380 of branched fatty acids than linear isomers.⁵³ This might lead to the underestimation of
381 the hTTR binding potency of tetradecyl benzenesulfonate in the environment. Future
382 studies are warranted to investigate isomer-specific binding of hydrocarbon surfactants
383 to hTTR.

384 Moreover, as discussed above (Figure 1b and 1c), we found that the hTTR and
385 FABP1 proteins may share common ligands in the tested indoor dust and sewage sludge
386 samples. Previously, we demonstrated that several hydrocarbon surfactants including
387 alkyl benzenesulfonate, alkyl sulfate, and alkyl sulfonate were predominant synthetic
388 ligands of FABP1 in indoor dust and sewage sludge samples.²⁶ Motivated by this, we
389 further included 11 hydrocarbon surfactants in the FITC-T₄ displacement assay to test
390 their hTTR binding activities (Table S4). These chemicals usually have high
391 background contaminations in the LC-MS instrument and thereby could be missed by
392 our original screening algorithm. Among the 11 tested hydrocarbon surfactants, four of
393 them including dodecyl sulfate (Figure 3c), tridecyl sulfate (Figure 3d),
394 tetradecanesulfonate (Figure 3e), and docusate (Figure 3f) showed relatively strong
395 binding activities towards the hTTR protein, with the IC₅₀ and REP values ranging from
396 9.39 to 14.5 μM and 0.0152 to 0.0234, respectively. In contrast, hydrocarbon surfactants
397 with a too short (e.g., C₂, C₇, and C₈) or too long (C₁₆ and C₁₈) carbon chain length
398 displayed weak or even no hTTR binding (IC₅₀ > 50 μM and REP < 0.005) (Figure S8
399 and Figure S9). We conducted molecular docking with AutoDock Vina³⁷ to predict the
400 binding mode of hydrocarbon surfactants to the hTTR protein, and included PFOS in
401 the docking analysis for comparison. As shown in Figure S10a, PFOS could fit into the
402 interior of the ligand binding pocket of hTTR with its sulfonic acid group protruding
403 towards the surface and its fluorinated tail adopting an extended conformation (binding
404 energy = -8.6 kcal/mol). Its sulfonic acid group formed a salt bridge with Lys15, which
405 was consistent with previous observations⁴⁵ and demonstrated the accuracy of the
406 molecular docking analysis. Then, by taking dodecyl benzenesulfonate (binding energy
407 = -6.5 kcal/mol) as an example, we found that alkyl benzenesulfonate interacted with
408 hTTR in a similar manner to PFOS, except that its hydrophobic tail bent inside the
409 pocket interior (Figure S10b). Dodecyl benzenesulfonate also formed a salt bridge with

410 Lys15' and hydrophobic contacts with Ala108, Thr119, Leu17, Leu110, Thr106',
 411 Ala108', Leu17' and Leu110'. An additional anion- π interaction was also found to form
 412 between Lys15 and the benzene ring. Since hydrophobic contacts play a vital role in
 413 stabilizing the binding orientation, we deduced that smaller hydrocarbon surfactants
 414 (<C₈) could not form strong enough hydrophobic interactions with hTTR and would
 415 thus act as weaker hTTR ligands. In contrast, the alkyl chain of larger (>C₁₆) surfactants
 416 may have difficulty fitting into the hTTR binding pocket, resulting in low binding
 417 affinities. The molecular docking analysis provided a plausible explanation for the
 418 structure-activity relationships (SAR) of hydrocarbon surfactants.
 419



420
 421 **Figure 3. Binding of six hydrocarbon surfactants to native hTTR protein purified**
 422 **from human plasma.** The binding activity was determined by a fluorescence

423 displacement assay. $N = 3$. All data were normalized to solvent control. REP: relative
424 potency to T₄.

425

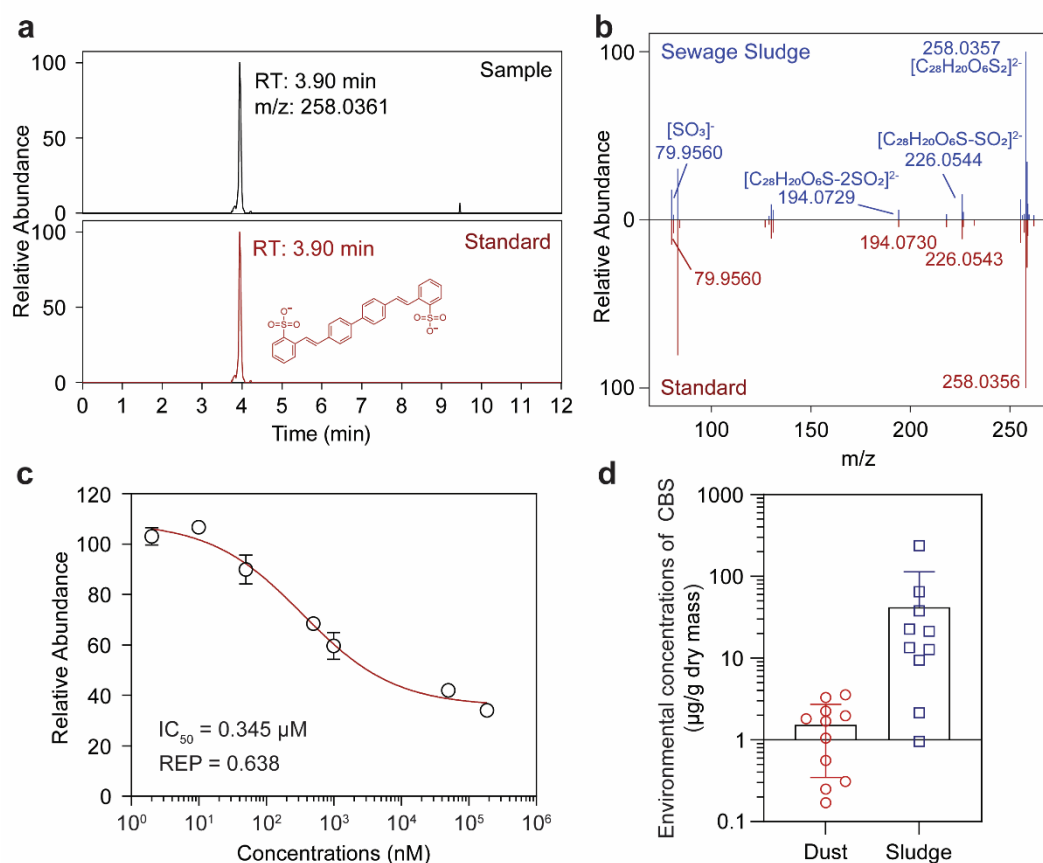
426 **Identification of a fluorescent brightener as a nM affinity hTTR binder.** Note
427 that only 3 of the 31 nonredundant putative hTTR ligands were identified through
428 database searching, probably because they were outside the TSCA or NORMAN
429 chemical libraries, or they were ionized in a unique way (*e.g.*, multiple charged ions).
430 We decided to employ *de novo* structural assignment for other putative hTTR ligands
431 beyond the initial suspect screening. The LC-MS feature with a m/z of 258.0361 and
432 retention time of 3.90 min attracted our attention since it was pulled-out both from
433 indoor dust and sewage sludge extracts with a marked fold change > 10 and P value $<$
434 0.001 . By carefully inspecting the isotopic distribution ($\Delta m/z = 0.5$ Da), this feature
435 was unexpectedly assigned as a doubly charged ion (Figure S11a). Its chemical formula
436 was assigned as $[C_{28}H_{20}O_6S_2]^{2-}$ with a mass error of 1.88 ppm. The MS² fragment of
437 $m/z = 79.9560$ (corresponding to $[SO_3]^-$) further suggested it was a sulfonate. The
438 sequential neutral loss of two SO₂ (*i.e.*, $m/z = 226.0544$ $[C_{28}H_{20}O_6S_2-SO_2]^{2-}$ and $m/z =$
439 194.0730 $[C_{28}H_{20}O_6S_2-2SO_2]^{2-}$) clearly demonstrated the presence of two sulfonate
440 groups in the molecule. By re-searching against the NORMAN Suspect List Exchange
441 database using the double charge³⁵, it was identified as CBS (CASRN: 27344-41-8). To
442 confirm its identity, we purchased the authentic standard (purity $> 99\%$). As illustrated
443 in Figure 4a and 4b, the RT and the MS² spectrum of the feature pulled-out from the
444 sample extracts matched exactly with the authentic standard of CBS, confirming the
445 identity of $m/z = 258.0361$. In addition to CBS, we also detected four additional doubly
446 charged chemicals in the indoor dust samples (Figure S11b to e). However, we were
447 not able to assign their structures because they were outside the TSCA or NORMAN
448 chemical databases. The MS information of these pulled-out chemicals has been
449 uploaded to our “environmental Chemical-Protein Interaction Network (eCPIN)”
450 database (<https://penggroup.shinyapps.io/ecpin/>)²², which is freely accessible. It would
451 be very interesting for colleagues working in nontargeted analysis to assign the
452 structures of these unknown hTTR ligands, and check if these ligands are detected in

453 other samples of interest (*e.g.*, human cohort blood samples).

454 The structure of CBS is very unique compared to previously known hTTR ligands.
455 This was interesting and demonstrated that APNA could identify novel ligands with
456 completely new chemotypes. We moved forward to validate its bioactivity through the
457 FITC-T₄ displacement assay as mentioned above. Supporting the APNA results, a dose-
458 dependent reduction in fluorescence intensity was observed ([Figure 4c](#)) with an IC₅₀
459 value of 0.345 μM, which confirmed the strong interaction between CBS and the hTTR
460 protein. The REP value of CBS was determined to be 0.638, which was greater than
461 PFOS (REP 0.49) and all the hydrocarbon surfactants tested in this study ([Table S4](#)).
462 Through molecular docking, we found that the two sulfonate groups of the CBS
463 molecule could form two hydrogen bonds with Thr123' and Ser117', and one salt bridge
464 with Arg104' on each end of the hTTR ligand binding pocket (inner and entrance),
465 which resulted in a stable binding orientation with a binding energy of -9.9 kcal/mol
466 ([Figure S10c](#)). Moreover, hydrophobic contacts with Thr106', Ala108', Leu110',
467 Ala108, Leu110, and Leu17 were also found. The special binding mode of CBS
468 deriving from its unique doubly charged structure may provide an explanation for its
469 strong hTTR binding potency.

470 Then, to better understand the potential environmental occurrence of CBS, we
471 decided to quantify CBS in the selected dust and sludge samples. CBS was detected in
472 all 11 indoor dust and 10 sewage sludge samples, at 0.17 to 3.55 μg/g (median: 1.69
473 μg/g) in indoor dust and 0.96 to 238 μg/g (median: 17.4 μg/g) in sewage sludge ([Figure](#)
474 [4d](#) and [Table S5](#)). The concentrations of CBS were about 3~4 orders of magnitudes
475 higher than those of PFOS in the same samples, but ~10 times lower than those of
476 hydrocarbon surfactants.²⁶ Two very recent studies from the Zeng group reported the
477 occurrence of CBS in indoor dust and sludge collected from China.^{54, 55} The detected
478 concentrations of CBS in our study were comparable to the results from the Zeng et al
479 studies (dust: 0.059 to 4.04 μg/g; sludge: 0.013 to 8.35 μg/g). These results
480 demonstrated its ubiquitous presence in the environment.

481



482

483 **Figure 4. Identification of a previously unrecognized hTTR ligand.** (a) Liquid
 484 chromatograms of CBS from extract of sewage sludge or the authentic standard. (b)
 485 MS² spectra used to assign the structure of CBS. (c) Binding activities of CBS to hTTR
 486 determined by the FITC-T₄ displacement assay. *N* = 3. (d) Environmental
 487 concentrations of CBS in extracts from indoor dust or sewage sludge.

488

489 CBS belongs to a class of mass-produced dyestuff chemicals known as fluorescent
 490 brighteners (FBs)⁵⁶ and has long been widely used as an optical brightener for various
 491 detergents. According to the Consumer Product Information Database (CPID,
 492 <https://www.whatsinproducts.com/>), ~158 detergent products contain CBS, and its
 493 contents is typically around 0.1-1%.⁵⁷ Furthermore, CBS has also been found in one
 494 rice noodle product at approximately 2.1 mg/kg in Korea.⁵⁸ These results suggested a
 495 clear potential for human exposure to CBS. However, the current toxicity information
 496 on CBS is surprisingly scarce. A recent study found that exposure to CBS could inhibit
 497 the enzyme activity of iodotyrosine deiodinase (IYD), which is an important iodide
 498 recycling enzyme for thyroid hormone synthesis.⁵⁹ Together with the information
 499 regarding its high hTTR binding affinity, IYD inhibition, close human contact, and high

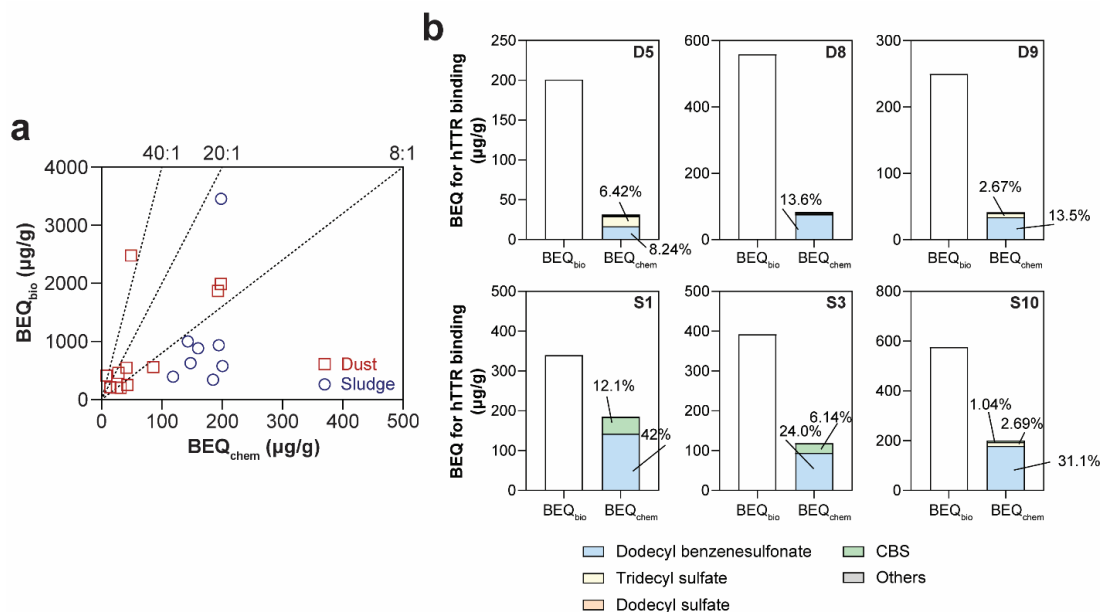
500 environmental concentrations, CBS might be an important TDC that has been
501 overlooked in previous studies. Future studies are warranted to clarify the potential
502 health effects of exposure to CBS in humans.

503

504 **Contributions of identified chemicals to total hTTR binding activities.** The BEQ
505 concept was used to determine the contributions towards hTTR activity in this study.⁶⁰
506 Four identified hTTR ligands by APNA (i.e., PFOS, dodecyl benzenesulfonate,
507 tetradecyl benzenesulfonate, and CBS) and nine hydrocarbon surfactants which
508 exhibited hTTR binding activities (Table S4) in the FITC-T₄ displacement assay were
509 included. The concentrations of CBS, tetradecyl benzenesulfonate, octyl sulfate, 2-
510 ethylhexyl sulfate, heptanesulfonate, and octanesulfonate in indoor dust and sewage
511 sludge samples were measured by constructing external calibration curves with
512 commercially available standards ($R^2 > 0.99$), while those of the other chemicals were
513 adopted directly from our previous study.²⁶ Then, by using the REP (Table S4) values
514 and the detected chemical concentrations (Table S5), BEQ_{chem} was calculated (eq 3) for
515 each sample with T₄ as the reference compound. By comparing the BEQ_{bio} and BEQ_{chem}
516 values, the detected chemicals could explain 1.92 to 17.1% (median: 9.95%) and 5.74
517 to 54.4% (median: 22.5%) of hTTR binding activities in dust and sludge samples,
518 respectively. The contributions of the detected chemicals to the total hTTR effect were
519 shown in Figure 5a and Table S6. Notably, in some samples, the detected chemicals
520 could explain >30% of the hTTR effects (e.g., 54.4% explained in sludge sample S1),
521 which was mostly driven by dodecyl benzenesulfonate and CBS (Figure 5b). This
522 mainly resulted from their extremely high concentrations in the environment (at mg/g
523 level for dodecyl benzenesulfonate)²⁶ or potent biological activity toward hTTR (REP
524 0.345 for CBS). In contrast, PFOS, which has been the subject of extensive research
525 attention, only contributed to <0.0001% of the total effects (Table S6). These results
526 were highly intriguing as only 1.2% of hTTR activities could be explained previously
527 by known hTTR ligands in indoor dust.¹⁷ Note that the contributions of hydrocarbon
528 surfactants to hTTR binding activities might be largely underestimated due to the lack
529 of authentic standards for most homologue/isomer compounds. Thus, we concluded

530 that hydrocarbon surfactants (especially for hydrocarbon sulfonates) and CBS are the
531 major hTTR ligands in the environment.

532



533

534 **Figure 5.** Comparison of biological equivalent concentration from bioanalysis (BEQ_{bio})
535 and chemical analysis (BEQ_{chem}) for hTTR binding activity (a). Red squares and blue
536 circles represent indoor dust and sewage sludge samples, respectively. Contributions of
537 identified hTTR ligands to the total hTTR binding activities in representative indoor
538 dust or sewage sludge samples were shown as bar plots (b). D represents indoor dust
539 samples, while S represents sewage sludge samples.

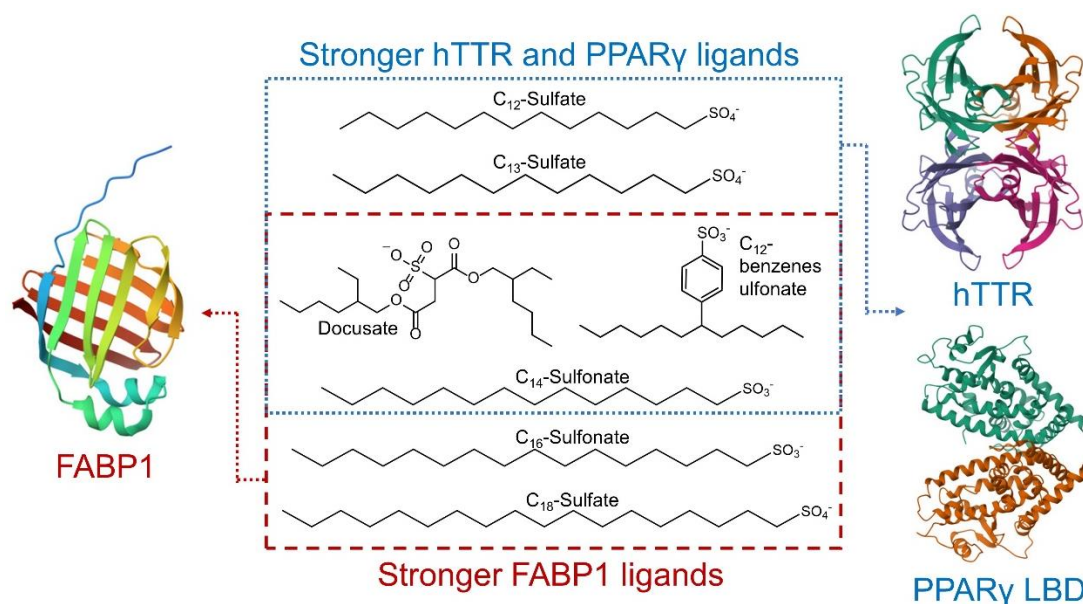
540

541 **Implications.** The incidence of thyroid-related disease including thyroid cancer have
542 rapidly increased over the last several decades.⁶¹ TDCs have long been hypothesized to
543 contribute to this increase, yet known TDCs cannot fully explain the related protein-
544 mediated activities. Indeed, known chemicals have been found to only explain ~1% of
545 the hTTR activity in the environment.¹⁷ Thus, it is important to identify the major TDCs
546 and investigate their potential contribution to thyroid-related disease. In this study, we
547 discovered that hydrocarbon sulfonates, including surfactants and a fluorescent
548 brightener, can explain a large portion of the hTTR activity in the environment.
549 Considering their high production volume, close human contact, and strong hTTR
550 potencies, it is important to investigate the potential health impacts of these two

551 compound families.

552 Due to their weak acute toxicities, hydrocarbon surfactants have long been
553 considered 'safe' chemicals, and very limited studies have investigated their chronic
554 toxicities. Recently, they were found to induce stronger toxicity to zebrafish embryo
555 and terrestrial plants than PFAS.^{62, 63} In our previous study, we also demonstrated that
556 hydrocarbon surfactants are predominant synthetic ligands for human FABP1 and
557 PPAR γ proteins in the environment.²⁶ Here, we further revealed that hydrocarbon
558 surfactants can also target the hTTR protein (Figure 6), indicating that hydrocarbon
559 surfactants may interfere with multiple biological processes within organisms.
560 Moreover, another European group also independently identified hydrocarbon
561 surfactants as hTTR ligands in treated wastewater and its downstream water, which
562 further validated our results and indicated the wide presence of hydrocarbon surfactants
563 in the environment. A major limitation of the current study is that *in vivo* metabolism
564 and elimination of hydrocarbon sulfonates were not taken into consideration.
565 Considering the close contact of these compounds with humans, *in vivo* animal testing
566 and epidemiological studies are warranted in the future to systematically assess their
567 chemical safety.

568



569

570 **Figure 6.** Binding of hydrocarbon surfactants to three human proteins with distinct
571 preference.

572 **Supporting Information Available**

573 The supporting information provides text, tables, and figures addressing: (1)
574 Supplementary materials and methods; (2) Validation of the FITC-T₄ probe; (3)
575 Validation of the displacement assay; (4) hTTR binding activities of indoor dust and
576 sewage sludge samples; (5) Correlation between hTTR and PPAR γ LBD activities; (6)
577 Verification of the recombinant His-tagged hTTR protein; (7) Benchmarking of the
578 APNA method; (8) hTTR binding activities of hydrocarbon surfactants; (9)
579 Relationship between carbon chain length and hTTR activity; (10) Molecular docking;
580 (11) Isotopic distributions of the doubly charged ions; (12) List of standards; (13) IC₅₀
581 and BEQ_{bio} values of environmental samples; (14) List of pulled-out LC-MS features;
582 (15) IC₅₀ and REP values of tested chemicals; (16) Environmental concentrations of
583 CBS and hydrocarbon surfactants; (17) Contributions of identified chemicals to the
584 total hTTR binding activities.

585

586 **Acknowledgements**

587 This work was supported by the Ontario Early Researcher Award, and NSERC
588 Discovery Grant. The authors also acknowledge the support of instrumentation grants
589 from the Canada Foundation for Innovation, the Ontario Research Fund, and the
590 NSERC Research Tools and Instrument Grant.

591

592

593 **References**

- 594 (1) Murk, A. J.; Rijntjes, E.; Blaauboer, B. J.; Clewell, R.; Crofton, K. M.; Dingemans, M. M. L.;
595 David Furlow, J.; Kavlock, R.; Köhrle, J.; Opitz, R.; Traas, T.; Visser, T. J.; Xia, M.; Gutleb, A. C.,
596 Mechanism-based testing strategy using *in vitro* approaches for identification of thyroid hormone
597 disrupting chemicals. *Toxicol. in Vitro* **2013**, *27*, (4), 1320-1346. DOI: 10.1016/j.tiv.2013.02.012.
- 598 (2) Haddow, J. E.; Palomaki, G. E.; Allan, W. C.; Williams, J. R.; Knight, G. J.; Gagnon, J.; O'Heir,
599 C. E.; Mitchell, M. L.; Hermos, R. J.; Waisbren, S. E.; Faix, J. D.; Klein, R. Z., Maternal thyroid
600 deficiency during pregnancy and subsequent neuropsychological development of the child. *N. Engl. J.*
601 *Med.* **1999**, *341*, (8), 549-555. DOI: 10.1056/NEJM199908193410801.
- 602 (3) de Jong, F. J.; Masaki, K.; Chen, H.; Remaley, A. T.; Breteler, M. M.; Petrovitch, H.; White,
603 L. R.; Launer, L. J., Thyroid function, the risk of dementia and neuropathologic changes: the Honolulu-
604 Asia aging study. *Neurobiol. Aging* **2009**, *30*, (4), 600-6. DOI: 10.1016/j.neurobiolaging.2007.07.019.
- 605 (4) Han, X.; Meng, L.; Li, Y.; Li, A.; Turyk, M. E.; Yang, R.; Wang, P.; Xiao, K.; Li, W.; Zhao, J.;
606 Zhang, Q.; Jiang, G., Associations between exposure to persistent organic pollutants and thyroid function
607 in a case-control study of east China. *Environ. Sci. Technol.* **2019**, *53*, (16), 9866-9875. DOI:
608 10.1021/acs.est.9b02810.
- 609 (5) Sun, Y.; Xia, P.-F.; Korevaar, T. I. M.; Mustieles, V.; Zhang, Y.; Pan, X.-F.; Wang, Y.-X.;
610 Messerlian, C., Relationship between blood trihalomethane concentrations and serum thyroid function
611 measures in U.S. adults. *Environ. Sci. Technol.* **2021**, *55*, (20), 14087-14094. DOI:
612 10.1021/acs.est.1c04008.
- 613 (6) Liu, M.; Li, A.; Meng, L.; Zhang, G.; Guan, X.; Zhu, J.; Li, Y.; Zhang, Q.; Jiang, G., Exposure
614 to novel brominated flame retardants and organophosphate esters and associations with thyroid cancer
615 risk: A case-control study in eastern China. *Environ. Sci. Technol.* **2022**, *56*, (24), 17825-17835. DOI:
616 10.1021/acs.est.2c04759.
- 617 (7) Hallgren, S.; Darnerud, P. O., Polybrominated diphenyl ethers (PBDEs), polychlorinated
618 biphenyls (PCBs) and chlorinated paraffins (CPs) in rats—testing interactions and mechanisms for
619 thyroid hormone effects. *Toxicology* **2002**, *177*, (2), 227-243. DOI: 10.1016/S0300-483X(02)00222-6.
- 620 (8) Darnerud, P. O.; Morse, D.; Klasson-Wehler, E.; Brouwer, A., Binding of a 3,3',4,4'-
621 tetrachlorobiphenyl (CB-77) metabolite to fetal transthyretin and effects on fetal thyroid hormone levels
622 in mice. *Toxicology* **1996**, *106*, (1), 105-114. DOI: 10.1016/0300-483X(95)03169-G.
- 623 (9) Kim, S. Y.; Choi, E.-S.; Lee, H.-J.; Moon, C.; Kim, E., Transthyretin as a new transporter of
624 nanoparticles for receptor-mediated transcytosis in rat brain microvessels. *Colloids Surf., B* **2015**, *136*,
625 989-996. DOI: 10.1016/j.colsurfb.2015.10.050.
- 626 (10) Meerts, I. A. T. M.; Assink, Y.; Ceniijn, P. H.; van den Berg, J. H. J.; Weijers, B. M.; Bergman,
627 Å.; Koeman, J. H.; Brouwer, A., Placental transfer of a hydroxylated polychlorinated biphenyl and effects
628 on fetal and maternal thyroid hormone homeostasis in the rat. *Toxicol. Sci.* **2002**, *68*, (2), 361-371. DOI:
629 10.1093/toxsci/68.2.361.
- 630 (11) Diamanti-Kandarakis, E.; Bourguignon, J.-P.; Giudice, L. C.; Hauser, R.; Prins, G. S.; Soto, A.
631 M.; Zoeller, R. T.; Gore, A. C., Endocrine-disrupting chemicals: An endocrine society scientific statement.
632 *Endocr. Rev.* **2009**, *30*, (4), 293-342. DOI: 10.1210/er.2009-0002.
- 633 (12) Meerts, I. A. T. M.; van Zanden, J. J.; Luijckx, E. A. C.; van Leeuwen-Bol, I.; Marsh, G.;
634 Jakobsson, E.; Bergman, Å.; Brouwer, A., Potent competitive interactions of some brominated flame
635 retardants and related compounds with human transthyretin *in vitro*. *Toxicol. Sci.* **2000**, *56*, (1), 95-104.
636 DOI: 10.1093/toxsci/56.1.95.

- 637 (13) Yang, X.; Ou, W.; Xi, Y.; Chen, J.; Liu, H., Emerging polar phenolic disinfection byproducts
638 are high-affinity human transthyretin disruptors: An *in vitro* and *in silico* study. *Environ. Sci. Technol.*
639 **2019**, *53*, (12), 7019-7028. DOI: 10.1021/acs.est.9b00218.
- 640 (14) Grimm Fabian, A.; Lehmler, H.-J.; He, X.; Robertson Larry, W.; Duffel Michael, W., Sulfated
641 metabolites of polychlorinated biphenyls are high-affinity ligands for the thyroid hormone transport
642 protein transthyretin. *Environ. Health Perspect.* **2013**, *121*, (6), 657-662. DOI: 10.1289/ehp.1206198.
- 643 (15) Weiss, J. M.; Andersson, P. L.; Lamoree, M. H.; Leonards, P. E. G.; van Leeuwen, S. P. J.;
644 Hamers, T., Competitive binding of poly- and perfluorinated compounds to the thyroid hormone transport
645 protein transthyretin. *Toxicol. Sci.* **2009**, *109*, (2), 206-216. DOI: 10.1093/toxsci/kfp055.
- 646 (16) Huang, K.; Wang, X.; Zhang, H.; Zeng, L.; Zhang, X.; Wang, B.; Zhou, Y.; Jing, T., Structure-
647 directed screening and analysis of thyroid-disrupting chemicals targeting transthyretin based on
648 molecular recognition and chromatographic separation. *Environ. Sci. Technol.* **2020**, *54*, (9), 5437-5445.
649 DOI: 10.1021/acs.est.9b05761.
- 650 (17) Hamers, T.; Kortenkamp, A.; Scholze, M.; Molenaar, D.; Cenijn, P. H.; Weiss, J. M.,
651 Transthyretin-binding activity of complex mixtures representing the composition of thyroid-hormone
652 disrupting contaminants in house dust and human serum. *Environ. Health Perspect.* **2020**, *128*, (1),
653 017015. DOI: 10.1289/EHP5911.
- 654 (18) Wang, Z.; Walker, G. W.; Muir, D. C. G.; Nagatani-Yoshida, K., Toward a global
655 understanding of chemical pollution: A first comprehensive analysis of national and regional chemical
656 inventories. *Environ. Sci. Technol.* **2020**, *54*, (5), 2575-2584. DOI: 10.1021/acs.est.9b06379.
- 657 (19) Tian, Z.; Zhao, H.; Peter Katherine, T.; Gonzalez, M.; Wetzel, J.; Wu, C.; Hu, X.; Prat, J.;
658 Mudrock, E.; Hettinger, R.; Cortina Allan, E.; Biswas Rajshree, G.; Kock Flávio Vinicius, C.; Soong, R.;
659 Jenne, A.; Du, B.; Hou, F.; He, H.; Lundeen, R.; Gilbreath, A.; Sutton, R.; Scholz Nathaniel, L.; Davis
660 Jay, W.; Dodd Michael, C.; Simpson, A.; McIntyre Jenifer, K.; Kolodziej Edward, P., A ubiquitous tire
661 rubber-derived chemical induces acute mortality in coho salmon. *Science* **2021**, *371*, (6525), 185-189.
662 DOI: 10.1126/science.abd6951.
- 663 (20) Jonkers, T. J. H.; Meijer, J.; Vlaanderen, J. J.; Vermeulen, R. C. H.; Houtman, C. J.; Hamers,
664 T.; Lamoree, M. H., High-performance data processing workflow incorporating effect-directed analysis
665 for feature prioritization in suspect and nontarget screening. *Environ. Sci. Technol.* **2022**, *56*, (3), 1639-
666 1651. DOI: 10.1021/acs.est.1c04168.
- 667 (21) Weiss, J. M.; Andersson, P. L.; Zhang, J.; Simon, E.; Leonards, P. E. G.; Hamers, T.; Lamoree,
668 M. H., Tracing thyroid hormone-disrupting compounds: database compilation and structure-activity
669 evaluation for an effect-directed analysis of sediment. *Anal. Bioanal. Chem.* **2015**, *407*, (19), 5625-5634.
670 DOI: 10.1007/s00216-015-8736-9.
- 671 (22) Gong, Y.; Yang, D.; Barrett, H.; Sun, J.; Peng, H. Building the environmental chemical-protein
672 interaction network (eCPIN): An exposome-wide strategy for bioactive chemical contaminant
673 identification. *Environ. Sci. Technol.* **2023**, *57*, (9), 3486-3495. DOI: 10.1021/acs.est.2c02751.
- 674 (23) Peng, H.; Sun, J. X.; Alharbi, H. A.; Jones, P. D.; Giesy, J. P.; Wiseman, S. Peroxisome
675 proliferator-activated receptor gamma is a sensitive target for oil sands process-affected water: effects on
676 adipogenesis and identification of ligands. *Environ. Sci. Technol.* **2016**, *50*, (14), 7816-7824. DOI:
677 10.1021/acs.est.6b01890.
- 678 (24) Yang, D.; Liu, Q.; Wang, S.; Bozorg, M.; Liu, J.; Nair, P.; Balaguer, P.; Song, D.; Krause, H.;
679 Ouazia, B.; Abbatt, J. P. D.; Peng, H., Widespread formation of toxic nitrated bisphenols indoors by
680 heterogeneous reactions with HONO. *Sci. Adv.* **2022**, *8*, (48), eabq7023. DOI: 10.1126/sciadv.abq7023.

- 681 (25) Liu, J. B.; Sahin, C.; Ahmad, S.; Magomedova, L.; Zhang, M. H.; Jia, Z. P.; Metherel, A. H.;
682 Orellana, A.; Poda, G.; Bazinet, R. P.; Attisano, L.; Cummins, C. L.; Peng, H.; Krause, H. M. The omega-
683 3 hydroxy fatty acid 7(S)-HDHA is a high-affinity PPAR α ligand that regulates brain neuronal
684 morphology. *Sci. Signaling* **2022**, *15*, (741), eabo1857. DOI: 10.1126/scisignal.abo1857.
- 685 (26) Gong, Y.; Yang, D.; Liu, J.; Barrett, H.; Sun, J.; Peng, H., Disclosing environmental ligands of
686 L-FABP and PPAR γ : Should we re-evaluate the chemical safety of hydrocarbon surfactants? *Environ.*
687 *Sci. Technol.* **2023**, *57*, (32), 11913-11925. DOI: 10.1021/acs.est.3c02898.
- 688 (27) Yang, D.; Han, J.; Hall, D. R.; Sun, J.; Fu, J.; Kutarna, S.; Houck, K. A.; LaLone, C. A.;
689 Doering, J. A.; Ng, C. A.; Peng, H., Nontarget screening of per- and polyfluoroalkyl substances binding
690 to human liver fatty acid binding protein. *Environ. Sci. Technol.* **2020**, *54*, (9), 5676-5686. DOI:
691 10.1021/acs.est.0c00049.
- 692 (28) Barrett, H.; Sun, J.; Gong, Y.; Yang, P.; Hao, C.; Verreault, J.; Zhang, Y.; Peng, H., Triclosan
693 is the predominant antibacterial compound in Ontario sewage sludge. *Environ. Sci. Technol.* **2022**, *56*,
694 (21), 14923-14936. DOI: 10.1021/acs.est.2c00406.
- 695 (29) Sun, J.; Barrett, H.; Hall, D. R.; Kutarna, S.; Wu, X.; Wang, Y.; Peng, H., Ecological role of
696 6OH-BDE47: Is it a chemical offense molecule mediated by enoyl-ACP reductases? *Environ. Sci.*
697 *Technol.* **2022**, *56*, (1), 451-459. DOI: 10.1021/acs.est.1c05718.
- 698 (30) Ren, X. M.; Guo, L.-H., Assessment of the binding of hydroxylated polybrominated diphenyl
699 ethers to thyroid hormone transport proteins using a site-specific fluorescence probe. *Environ. Sci.*
700 *Technol.* **2012**, *46*, (8), 4633-4640. DOI: 10.1021/es2046074.
- 701 (31) Smith, D., Enhancement fluoroimmunoassay of thyroxine. *FEBS lett.* **1977**, *77*, (1), 25-27.
- 702 (32) Kutarna, S.; Tang, S.; Hu, X.; Peng, H., Enhanced nontarget screening algorithm reveals highly
703 abundant chlorinated azo dye compounds in house dust. *Environ. Sci. Technol.* **2021**, *55*, (8), 4729-4739.
704 DOI: 10.1021/acs.est.0c06382.
- 705 (33) Smith, C. A.; Want, E. J.; O'Maille, G.; Abagyan, R.; Siuzdak, G. XCMS: Processing mass
706 spectrometry data for metabolite profiling using nonlinear peak alignment, matching, and identification.
707 *Anal. Chem.* **2006**, *78*, (3), 779-787. DOI: 10.1021/ac051437y.
- 708 (34) EPA, U. S. TSCA Chemical Substance Inventory. <https://www.epa.gov/tsca-inventory>
709 (accessed 2023-12-16).
- 710 (35) NORMAN Home Page. <https://www.norman-network.com/nds/SLE/> (accessed 2023-12-16).
- 711 (36) Schymanski, E. L.; Jeon, J.; Gulde, R.; Fenner, K.; Ruff, M.; Singer, H. P.; Hollender, J.,
712 Identifying small molecules via high resolution mass spectrometry: Communicating confidence. *Environ.*
713 *Sci. Technol.* **2014**, *48*, (4), 2097-2098. DOI: 10.1021/es5002105.
- 714 (37) Trott, O.; Olson, A. J., AutoDock Vina: Improving the speed and accuracy of docking with a
715 new scoring function, efficient optimization, and multithreading. *J. Comput. Chem.* **2010**, *31*, (2), 455-
716 461. DOI: 10.1002/jcc.21334.
- 717 (38) Ouyang, X.; Froment, J.; Leonards, P. E. G.; Christensen, G.; Tollefsen, K.-E.; de Boer, J.;
718 Thomas, K. V.; Lamoree, M. H., Miniaturization of a transthyretin binding assay using a fluorescent
719 probe for high throughput screening of thyroid hormone disruption in environmental samples.
720 *Chemosphere* **2017**, *171*, 722-728. DOI: 10.1016/j.chemosphere.2016.12.119.
- 721 (39) Cao, J.; Lin, Y.; Guo, L.-H.; Zhang, A.-Q.; Wei, Y.; Yang, Y., Structure-based investigation on
722 the binding interaction of hydroxylated polybrominated diphenyl ethers with thyroxine transport proteins.
723 *Toxicology* **2010**, *277*, (1), 20-28. DOI: 10.1016/j.tox.2010.08.012.
- 724 (40) Suzuki, G.; Takigami, H.; Nose, K.; Takahashi, S.; Asari, M.; Sakai, S.-i., Dioxin-like and

725 transthyretin-binding compounds in indoor dusts collected from Japan: Average daily dose and possible
726 implications for children. *Environ. Sci. Technol.* **2007**, *41*, (4), 1487-1493. DOI: 10.1021/es061907l.

727 (41) Young Anna, S.; Zoeller, T.; Hauser, R.; James-Todd, T.; Coull Brent, A.; Behnisch Peter, A.;
728 Brouwer, A.; Zhu, H.; Kannan, K.; Allen Joseph, G., Assessing indoor dust interference with human
729 nuclear hormone receptors in cell-based luciferase reporter assays. *Environ. Health Perspect.* **2021**, *129*,
730 (4), 047010. DOI: 10.1289/EHP8054.

731 (42) Gracia-Lor, E.; Rousis, N. I.; Hernández, F.; Zuccato, E.; Castiglioni, S., Wastewater-based
732 epidemiology as a novel biomonitoring tool to evaluate human exposure to pollutants. *Environ. Sci.*
733 *Technol.* **2018**, *52*, (18), 10224-10226. DOI: 10.1021/acs.est.8b01403.

734 (43) Richieri, G. V.; Ogata, R. T.; Zimmerman, A. W.; Veerkamp, J. H.; Kleinfeld, A. M., Fatty acid
735 binding proteins from different tissues show distinct patterns of fatty acid interactions. *Biochemistry* **2000**,
736 *39*, (24), 7197-7204. DOI: 10.1021/bi000314z.

737 (44) Lim, C.-F.; Munro, S. L. A.; Wynne, K. N.; Topliss, D. J.; Stockigt, J. R., Influence of
738 nonesterified fatty acids and lysolecithins on thyroxine binding to thyroxine-binding globulin and
739 transthyretin. *Thyroid* **1995**, *5*, (4), 319-324. DOI: 10.1089/thy.1995.5.319.

740 (45) Xin, Y.; Ren, X.-M.; Ruan, T.; Li, C.-H.; Guo, L.-H.; Jiang, G., Chlorinated
741 polyfluoroalkylether sulfonates exhibit similar binding potency and activity to thyroid hormone transport
742 proteins and nuclear receptors as perfluorooctanesulfonate. *Environ. Sci. Technol.* **2018**, *52*, (16), 9412-
743 9418. DOI: 10.1021/acs.est.8b01494.

744 (46) Yang, X.; Lyakurwa, F.; Xie, H.; Chen, J.; Li, X.; Qiao, X.; Cai, X., Different binding
745 mechanisms of neutral and anionic poly-/perfluorinated chemicals to human transthyretin revealed by *in*
746 *silico* models. *Chemosphere* **2017**, *182*, 574-583. DOI: 10.1016/j.chemosphere.2017.05.016.

747 (47) Hill, K. L.; Mortensen, Å.-K.; Tedecheil, D.; Willmore, W. G.; Sylte, I.; Jenssen, B. M.;
748 Letcher, R. J., *In vitro* and *in silico* competitive binding of brominated polyphenyl ether contaminants
749 with human and gull thyroid hormone transport proteins. *Environ. Sci. Technol.* **2018**, *52*, (3), 1533-1541.
750 DOI: 10.1021/acs.est.7b04617.

751 (48) Bramwell, L.; Glinianaia, S. V.; Rankin, J.; Rose, M.; Fernandes, A.; Harrad, S.; Pless-Mulolli,
752 T., Associations between human exposure to polybrominated diphenyl ether flame retardants via diet and
753 indoor dust, and internal dose: A systematic review. *Environ. Int.* **2016**, *92-93*, 680-694. DOI:
754 10.1016/j.envint.2016.02.017.

755 (49) Andreu, V.; Picó, Y., Determination of linear alkylbenzenesulfonates and their degradation
756 products in soils by liquid chromatography-electrospray-ion trap multiple-stage mass spectrometry. *Anal.*
757 *Chem.* **2004**, *76*, (10), 2878-2885. DOI: 10.1021/ac035483e.

758 (50) Lara-Martín, P. A.; Gómez-Parra, A.; Sanz, J. L.; González-Mazo, E., Anaerobic degradation
759 pathway of linear alkylbenzene sulfonates (LAS) in sulfate-reducing marine sediments. *Environ. Sci.*
760 *Technol.* **2010**, *44*, (5), 1670-1676. DOI: 10.1021/es9032887.

761 (51) Riddell, N.; Arsenault, G.; Benskin, J. P.; Chittim, B.; Martin, J. W.; McAlees, A.; McCrindle,
762 R., Branched perfluorooctane sulfonate isomer quantification and characterization in blood serum
763 samples by HPLC/ESI-MS(MS). *Environ. Sci. Technol.* **2009**, *43*, (20), 7902-7908. DOI:
764 10.1021/es901261v.

765 (52) EPA, U. S. Chemical Data Reporting under the Toxic Substances Control Act.
766 <https://www.epa.gov/chemical-data-reporting> (accessed 2023-12-16).

767 (53) Hanhoff, T.; Benjamin, S.; Borchers, T.; Spener, F., Branched-chain fatty acids as activators
768 of peroxisome proliferator-activated receptors. *Eur. J. Lipid Sci. Technol.* **2005**, *107*, (10), 716-729. DOI:

769 10.1002/ejlt.200401076.
770 (54) Zeng, L.; Han, X.; Pang, S.; Ge, J.; Feng, Z.; Li, J.; Du, B., Nationwide occurrence and
771 unexpected severe pollution of fluorescent brighteners in the sludge of China: An emerging
772 anthropogenic marker. *Environ. Sci. Technol.* **2023**, *57*, (8), 3156-3165. DOI: 10.1021/acs.est.2c08491.
773 (55) Chen, H.; Han, X.; Zhu, C.; Du, B.; Tan, L.; He, R.; Shen, M.; Liu, L.-Y.; Zeng, L.,
774 Identification of fluorescent brighteners as another emerging class of abundant, ubiquitous pollutants in
775 the indoor environment. *Environ. Sci. Technol.* **2022**, *56*, (14), 10131-10140. DOI:
776 10.1021/acs.est.2c03082.
777 (56) Baoxu Chemical. Fluorescent Brightener Agent Definition & Classification.
778 <https://www.additivesforpolymer.com/fluorescent-brightener-definition-classificati/> (accessed 2023-12-
779 16).
780 (57) Consumer Product Information Database (CPID). Disodium Distyrylbiphenyl Disulfonate.
781 <https://www.whatsinproducts.com/chemicals/view/1/4359/027344-41-8> (accessed 2023-12-16).
782 (58) Ko, K. Y.; Lee, C. A.; Choi, J. C.; Kim, M., Determination of Tinopal CBS-X in rice papers
783 and rice noodles using HPLC with fluorescence detection and LC-MS/MS. *Food Addit Contam.: Part A*
784 **2014**, *31*, (9), 1451-9. DOI: 10.1080/19440049.2014.934302.
785 (59) Olker, J. H.; Korte, J. J.; Denny, J. S.; Haselman, J. T.; Hartig, P. C.; Cardon, M. C.; Hornung,
786 M. W.; Degitz, S. J., *In vitro* screening for chemical inhibition of the iodide recycling enzyme,
787 iodotyrosine deiodinase. *Toxicol. In Vitro* **2021**, *71*, 105073. DOI: 10.1016/j.tiv.2020.105073.
788 (60) Neale, P. A.; Ait-Aissa, S.; Brack, W.; Creusot, N.; Denison, M. S.; Deutschmann, B.;
789 Hilscherova, K.; Hollert, H.; Krauss, M.; Novak, J.; Schulze, T.; Seiler, T. B.; Serra, H.; Shao, Y.; Escher,
790 B. I., Linking *in vitro* effects and detected organic micropollutants in surface water using mixture-toxicity
791 modeling. *Environ. Sci. Technol.* **2015**, *49*, (24), 14614-24. DOI: 10.1021/acs.est.5b04083.
792 (61) Tang, Z.; Zhang, J.; Zhou, Q.; Xu, S.; Cai, Z.; Jiang, G., Thyroid cancer “Epidemic”: A socio-
793 environmental health problem needs collaborative efforts. *Environ. Sci. Technol.* **2020**, *54*, (7), 3725-
794 3727. DOI: 10.1021/acs.est.0c00852.
795 (62) Annunziato Kate, M.; Doherty, J.; Lee, J.; Clark John, M.; Liang, W.; Clark Christopher, W.;
796 Nguyen, M.; Roy Monika, A.; Timme-Laragy Alicia, R., Chemical characterization of a legacy aqueous
797 film-forming foam sample and developmental toxicity in zebrafish (*Danio rerio*). *Environ. Health*
798 *Perspect.* **2020**, *128*, (9), 097006. DOI: 10.1289/EHP6470.
799 (63) Wu, X.; Nguyen, H.; Kim, D.; Peng, H., Chronic toxicity of PFAS-free AFFF alternatives in
800 terrestrial plant *Brassica rapa*. *Sci. Total Environ.* **2022**, *850*, 158100. DOI:
801 10.1016/j.scitotenv.2022.158100.
802